Beyond Parameter Estimation: Extending Biomechanical Modeling by the Explicit Exploration of Model Topology

Francisco J. Valero-Cuevas*, *Member, IEEE*, Vikrant V. Anand, Anupam Saxena, and Hod Lipson, *Member, IEEE*

***Abstract*—Selecting a model topology that realistically predicts biomechanical function remains an unsolved problem. Today's dominant modeling approach is to replicate experimental input/output data by performing parameter estimation on an assumed topology. In contrast, we propose that modeling some complex biomechanical systems requires the explicit and simultaneous exploration of model topology (i.e., the type, number, and organization of physics-based functional building blocks) and parameter values. In this paper, we use the example of modeling the notoriously complex tendon networks of the fingers to present three critical advances towards the goal of implementing this extended modeling paradigm. First, we describe a novel computational environment to perform quasi-static simulations of arbitrary topologies of elastic structures undergoing large deformations. Second, we use this form of simulation to show that the assumed topology for the tendon network of a finger plays an important role in the propagation of tension to the finger joints. Third, we demonstrate the use of a novel inference algorithm that simultaneously explores the topology and parameter values for hidden synthetic tendon networks. We conclude by discussing critical issues of observability, separability, and uniqueness of topological features inferred from input/output data, and outline the challenges that need to be overcome to apply this novel modeling paradigm to extract causal models in real anatomical systems.**

***Index Terms*—Bioinformatics, biomechanical model, hand, machine learning.**

I. Introduction

ANALYTICAL and computational biomechanical models are traditionally constructed by using expert knowledge to approximate the observable functional anatomy by a mechanical structure, and then optimizing model parameters to fit measured biomechanical data (e.g., [1]–[4] and Fig. 1(a)). The inevitable discrepancies between model predictions and experimental data are, to a large extent, attributed to the variability and uncertainty in parameter values [5], [6].

More fundamentally, however, the validity and usefulness of the state-of-the-art modeling necessarily depends on whether the *structure* (i.e., *topology*) of the model (and not just model parameters) chosen by the expert(s) is appropriate to the research question. This has naturally led to valuable debates about the virtues of, for example, "simple" versus "complex" models, "generic" versus "subject or patient specific" models, or "deterministic" versus "probabilistic" models to name a few. In spite of numerous modeling efforts and successes in simulation, optimization, and computer-aided design (CAD)-like packages for biomechanical systems, assembling causal (i.e., functionally predictive) models where biomechanical function robustly emerges from the structure remains a challenging problem. Therefore, much work is directed at understanding the paradigm within which the state-of-the-art modeling is being carried out, and proposing means to extend it. For example, there is a healthy debate on alternative versions of muscle models [7], thumb [5], [6], or ankle [8] kinematics. In this paper, we propose a systematic means to improve modeling efforts by simultaneously exploring model structure and parameters.

The novel model inference approach we present here is based on the explicit distinction between model *topology* and *parameter values* [Fig. 1(b)]. Traditionally, models are defined *a priori* from expert knowledge, and then their parameters are adjusted. Although some parametric identification methods exist for automatically adjusting the parameters of these models [9]–[11], identifying the accurate topology will be difficult for modeling increasingly complex biomechanical systems. Here, we introduce a method to explore both the topology and parameters simultaneously. The *topology* of a model is its structure explicitly defined by the type, number, and organization of the *elementary building blocks* of the biomechanical description (i.e., tendons, muscles, bones, ligaments, pulleys, etc.) and is the unambiguous statement of the assumed biomechanical structure and the causal relationships assumed to be at work. The *parameters values* are the particulars associated with each building block (i.e., shape, size, strength, material properties, etc.), which define a particular instantiation of the assumed model topology [12]–[14]. Thus, a *model* is a particular instantiation of a topology with specific parameter values [13], [15] [Fig. 1(b)].

Importantly, in cases where noise is not a dominant artifact, an advantage of the model inference approach is that the in-

Manuscript received August 25, 2006; revised February 11, 2007. This work was supported in part by the National Science Foundation under Grants 0237258 (CAREER award) and 0312271 (ITR project) and the National Institutes of Health (NIH) under Grants AR050520 and AR052345. Its contents are solely the responsibility of the authors and do not necessarily represent the official views of the National Institute of Arthritis and Musculoskeletal and Skin Diseases (NIAMS) or the NIH. *Asterisk indicates corresponding author.*

*F. J. Valero-Cuevas is with the Neuromuscular Biomechanics Laboratory, Department of Biomedical Engineering and Division of Biokinesiology and Physical Therapy, University of Southern California, 3710 McClintock Avenue, Room RTH 402, Los Angeles, CA 90089 USA (e-mail: valero@usc.edu).

V. V. Anand and A. Saxena were with the Neuromuscular Biomechanics Laboratory and Computational Synthesis Laboratory, Sibley School of Mechanical and Aerospace Engineering, Cornell University, Ithaca, NY 14853 USA.

H. Lipson is with the Computational Synthesis Laboratory, Sibley School of Mechanical and Aerospace Engineering, Cornell University Ithaca, NY 14853 USA.

Color versions of one or more of the figures in this paper are available online at http://ieeexplore.ieee.org.

Digital Object Identifier 10.1109/TBME.2007.906494

0018-9294/$25.00 © 2007 IEEE

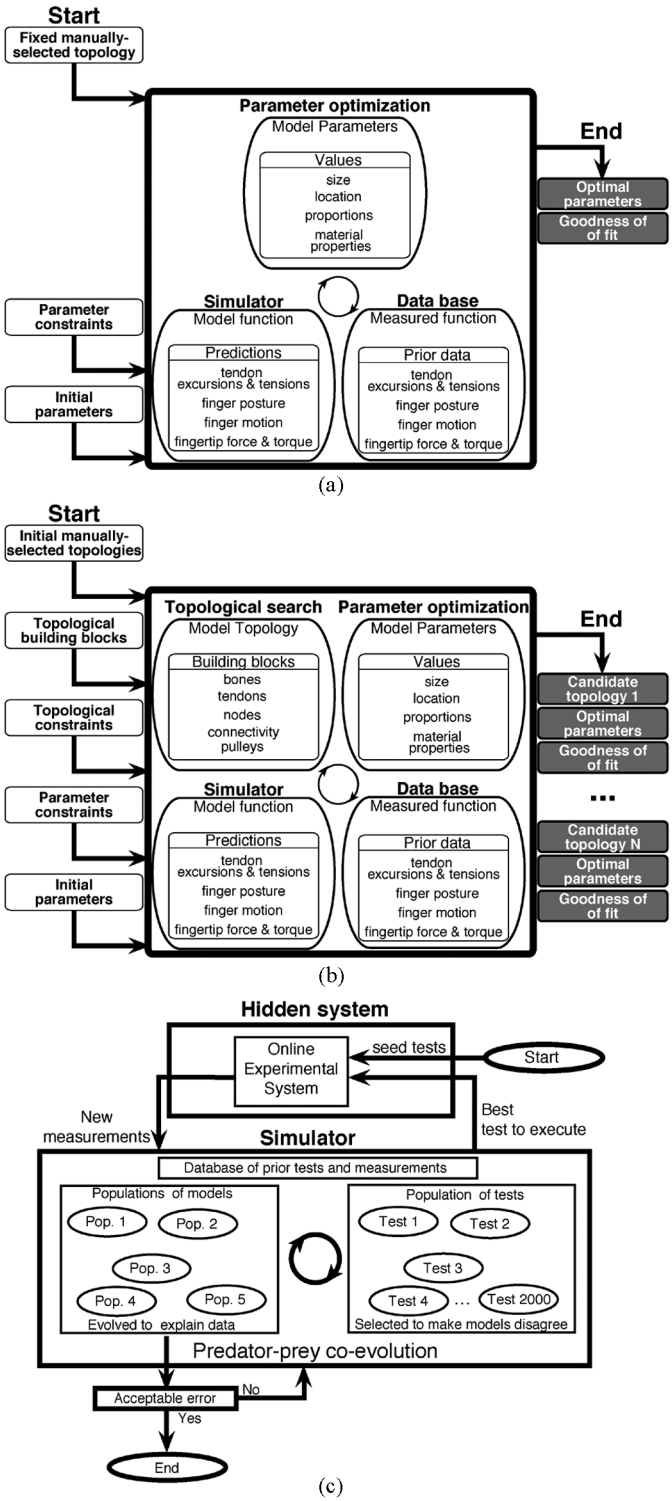


Fig. 1. Comparison between (a) optimization over the parameter space versus (b) optimization over the model space. Note that in (a) the topology of the model is assumed *a priori* and remains fixed, whereas in (b) both the topology and parameters can be adjusted to fit the data. Importantly, (b) can converge to a single or multiple models compatible with the data. (c) The estimation–exploration inference algorithm is an improvement on (b) using online sparse experimentation to execute only informative tests.

evitable discrepancies between predicted and measured data are now interpreted as either unsatisfactory parameter values, *inadequate model topology, or both* [13]. The modeling debate is thus enlarged to include whether additional or alternative explorations of the parameter values would improve results sufficiently, or if using an alternative model topology would be more fruitful, or even necessary [6], [13]. The search for an appropriate model then happens over the larger *model space*, which now encompasses the combination of the spaces of possible topologies *and* possible parameter values, both subject to anatomical and biomechanical constraints.

The focus of this paper is on functional models that provide insight into the biomechanical system's actual inner workings. This is in contrast to, say, a neural network model representation, which provides a mathematical mapping of inputs to outputs, but offers less insight into the structure and function of the real system. The objective of this paper is to present three following critical advances towards the goal of implementing this extended modeling paradigm using as examples 2-D and 3-D tendon networks analogous to those found in human fingers:

- describe a novel computational environment to perform quasi-static simulations of arbitrary topologies of elastic structures undergoing large deformations;
- use this form of simulation to show that the assumed topology for the tendon network of a fingers plays an important role in the propagation of tension to the finger joints;
- demonstrate the use of a novel inference algorithm that simultaneously explores the topology and parameter values for hidden synthetic tendon networks, with both random and intelligent testing.

Finally, we conclude by discussing critical issues of observability, separability, and uniqueness of topological features inferred from input/output data, and outline the challenges that need to be overcome to apply this novel modeling paradigm to extract causal models in real anatomical systems.

II. Methods

The proposed computational environment has the following characteristics: 1) it is designed to handle complex networks of elastic structures, such as the tendon networks in the fingers, 2) it uses a special quasi-static solver to find static equilibrium positions under known applied loads, 3) it permits simultaneous variation of model topology and model parameter values, and 4) it utilizes a stochastic optimization algorithm to search different combinations of model topology and model parameter values automatically, since stochastic algorithms are capable of handling discrete design variables such as those related to model topology.

A. Computational Environment to Describe and Simulate Biomechanical Models

1) Description of Anatomical Structures for Quasi-Static Simulation: To explore the problem of modeling the structure and function of the fingers, we have developed a biomechanical model simulator to describe the structure of arbitrary topological arrangements of fundamental musculoskeletal building blocks (Fig. 2; tendons, muscles, articular surfaces, bones, ligaments, and pulleys; [12], [13], [16]). Each building block is defined by its parameter values and described by a strain–stress relationship (which can be highly nonlinear) and a function that

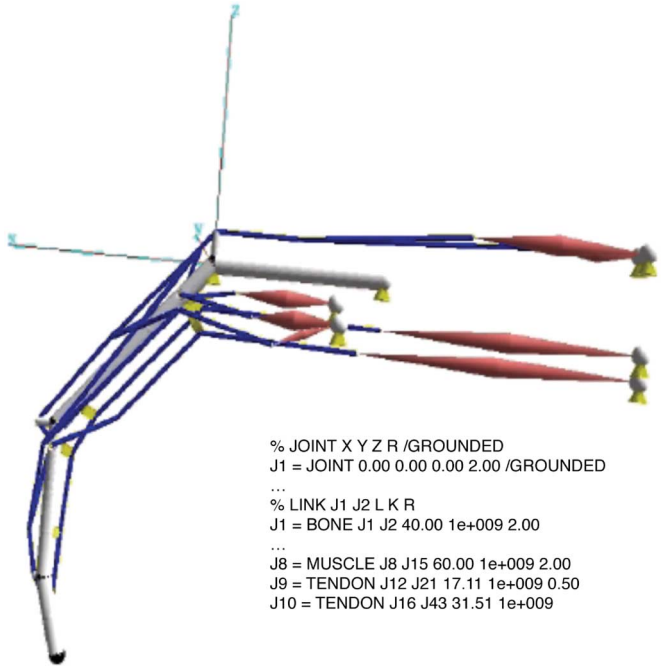


Fig. 2. Sample 3-D finger model in our simulator. The simulator uses a relaxation algorithm to predict the biomechanical function emerging from the topological layout of building blocks with specific parameter values. Given an input in the form of, say, changes in muscle tensions, the forward simulator predicts the new equilibrium 3-D posture of the finger. This schematic example contains all muscles of the index finger and tendinous interconnections as per Winslow's idealization of the extensor mechanism. This model is topologically equivalent to our 3-D finger model [36]. Like other CAD-like modeling environments, it can be easily described by a script language (inset), via a graphical user interface or autonomously via application programming interface.

relates strain to geometry (e.g., constant volume muscle). The simulator allows us to construct biomechanical models either interactively (through the graphical user interface in Fig. 2), through a biomechanical model script (see inset in Fig. 2), or through an application programming interface which allows external programs, such as a computational inference algorithm, to describe and solve biomechanical models automatically. Fig. 2 shows the example of a topologically plausible schematic biomechanical model of the index finger. Joint axes define the ball-and-socket, saddle-shaped, hinge, and sliding joints.

2) Causal Interaction Among Anatomical Structures (Quasi-Static Forward Simulation): In our simulator, the biomechanical function of the system emerges from the topological layout, size, and organization among building blocks. The simulator uses a novel relaxation-based approach for solving the kinematic motion of compound nonlinear mechanisms with multiple entangled kinematic chains [25]. The simulator accounts for quasi-static viscous-like motion ("pseudo" or "first-order" dynamics) but ignores dynamic effects. This property is specifically well suited to the simulation of hand function during everyday multifinger manipulation. Numerous studies have established that the fingers are damped systems where inertial effects are only important for high-speed trilling motions or tremors not seen in every day manipulation tasks (e.g., [17]–[22]). The biomechanical descriptions in our models are functional (i.e., simulatable) in the strict sense that we can predict the following: 1) the new equilibrium 3-D posture the finger will assume for a given change in muscle actuation if allowed to move (be it driven by tendon tensions or excursions), 2) the endpoint, joint, tendon pulley, and tendon forces for a given change in muscle force if constrained not to move, or 3) external loads applied anywhere on the structure.

The forward simulation process for biomechanical systems uses a relaxation solver similar to that used for design automation of robotic structures [23]. For a detailed description of the relaxation solver, please see [24]. Briefly, the algorithm performs iterations in response to applied loads or muscle forces until equilibrium is reached. Each iteration has two stages: computation of loads on elements and then computation of displacements at nodes to reach local equilibrium. A "node" is the connection between two or more elements, such as joints (connecting two bones), tendon insertions (connecting a tendon to a bone), or tendon junctions (connection tendons). The force-computation stage looks at each element of the structure and uses an element-specific mathematical model to compute residual forces in that element at its current state. For example, a tendon might behave elastically if it is in a state of tension, but might exert no force if in compression. In the second stage, all loads are accumulated at each of the structure nodes and node displacements are calculated using node-specific mathematical models. For example, a node representing a junction between three tendons might move freely in the direction of the resultant force being applied to it. The exact amount of displacement can be estimated from the stiffness of the node, derived from the stiffness of the elements connected to it. These cycles are iterated until all calculated node displacements are below the numerical threshold for negligible displacements. The relaxation process finds local equilibria, and by propagating loads and displacements, equilibrium is reached. If elements are well behaved (i.e., monotonic: smaller displacements produce smaller loads, and conversely, smaller loads produce smaller displacements), then the biomechanical model is guaranteed to reach equilibrium after a finite number of steps. However, there might be more than one equilibrium configuration. The simulation will find an equilibrium state that the biomechanical model can reach through successive incremental adaptations from the initial configuration.

B. Inference of Planar Hidden Networks via a Genetic Algorithm That Searches the Model Space

The problem of inferring an arbitrary network of elastic strings is one of system identification. In our prior work [15], [16], [25], we used a genetic algorithm to infer both, the topology and parameter values for models that emulate the propagation of tensions in a hidden network of strings. The data is obtained through testing of the "target" or "hidden" system, which in this work is a simulated (synthetic) tendon network hidden in a "black box." A *test* or *data point* is defined as a set of forces applied at prespecified "input" nodes on the target network and the resulting reaction forces at grounded "output" nodes. Those forces are applied and the target network is relaxed to equilibrium using the method described previously. In the "A" network shown in the top part of Fig. 5, for example, the input force is applied at the apex and the output forces are reaction forces at the grounded bottom nodes.

The inference algorithm sequentially tests the target system, adds the data point to the database, and evolves models to explain the latest data point in addition to all prior data points. The figure-of-merit attached to each model (its "fitness") corresponds to the largest error in matching the set of data points seen so far. The models are evolved until the fitness remains stagnant for 50 generations, at which point a new experiment (i.e., loading test) is performed on the black box and a new data point is added. The choice of experiments is described in the following for each portion of our work.

The models space is searched using a genetic algorithm, to find the best model (topology and parameters) that matches data points generated by tests so far. Note that while there are a number of optimization techniques that could be used, genetic (and other) stochastic algorithms are capable of handling discrete design variables due to, for example, severe discontinuities when a string is added to or removed from the network. In contrast, gradient-based optimization algorithms only work with continuous design variables when computation of the objective gradients is possible [15], [16], [25].

1) Genetic Encoding of the Network: In the genetic algorithm, each individual is a network of 25 nodes arranged in a regular 5×5 layout, and connected by 72 horizontal, vertical, and diagonal links. Thus, each individual resembles the meshes shown in the bottom part of Fig. 5. A direct encoding (i.e., representation) is used; the genotype and phenotype are the same. Depending on the problem, different nodes are grounded. Cables only connect at circled nodes.

The dimensions of the individuals, as well as the positions of their input and grounded nodes, match those of the target network. If the target fits within a rectangle of dimension $n \times m$ of arbitrary length units, the mesh dimensions will also be $n \times m$. Also, input forces are applied to the same location in both the target system and the meshes. If the target system has an input node at the Cartesian location (x, y), then the mesh, in its resting configuration, must have a node at (x, y) at which an input force can be applied. Finally, if the target system has a grounded node at location (x', y'), then the models must also have a grounded node at the same location. The position of all internal nodes in the target network is unknown.

The variables of the model are the resting (free) lengths of the links. In any particular problem, the set of grounded nodes remains constant, as do the values of E and A, the elastic modulus and cross-sectional area of the links. Thus, the functional behavior of the network is determined entirely by the resting lengths of the links in the network, and the genetic operators operate exclusively on these resting lengths. The input loads to this system (i.e., tests) are applied at the bottom three nodes (bottom of Fig. 5) and may vary in magnitude and direction (so long as they point downwards).

2) Fitness: The fitness of an individual (i.e., model) in a population is a function of the error between the output predictions of that individual for a series of tests and the actual outputs observed from the target network on the same series of tests. To calculate the fitness of an individual in the population, the data obtained from the "real" (black box) target system are used. Each data point has the form

$$(\{F_{i1}, F_{i2}, \ldots\}, \{F_{o1}, F_{o2}, \ldots\})$$

where the F_i's are input forces applied to the target network and the F_o's are the output forces observed at the grounded nodes.

The input forces from a data point are applied to the individual whose fitness is being calculated. That individual is then brought to its static equilibrium configuration using the relaxation method described previously. The residual forces at the grounded nodes are then stored as

$$\{F'_{o1}, F'_{o2}, \ldots\}.$$

Since the target network and the individuals have the same dimensions and identical locations of input and output nodes, the force outputs of a highly fit individual should match those of the target network. The difference between actual and predicted forces constitutes the error of the network for that data point. The error for data point p, ε_p, is given by

$$\varepsilon_p = \sum_{i=1}^{n} \frac{\left|\overrightarrow{F'_{oi}} - \overrightarrow{F_{oi}}\right|}{\left|\overrightarrow{F_{oi}}\right|}$$

where n is the number of output (grounded) nodes in the network, F' is the force predicted by the model, and F is the force observed in the target system. Note that the forces are vector quantities. Therefore, if F' and F have equal magnitude but different direction, the error will be nonzero. Also note that the error contribution from each output force is normalized.

The total error for the network is a weighted contribution of the average error and the maximum error calculated over all the data points

$$\varepsilon_{\text{total}} = \frac{1}{2} \cdot \overline{\varepsilon_p} + \frac{1}{2} \cdot \text{Max}(\varepsilon_p).$$

The fitness is defined to be

$$\text{Fitness} = 1.0 - \varepsilon_{\text{total}}.$$

3) Genetic Operators: The selection method used is deterministic crowding, which is one way to maintain population diversity [26]. The mutation operator performs point mutations by modifying the resting length of randomly chosen links in the network. The existing length is incremented by a number drawn from a normal distribution with a mean of zero. A two-point crossover operator is used; it chooses two nodes at random in the parents and swaps all the links in the patch between those nodes.

C. Simulating Two Alternative 3-D Tendinous Networks to Demonstrate Sensitivity to Model Topology

To demonstrate how the choice of topology affects the transmission of tendon tension, we present simulations of two alternative, yet tenable, topologies of the extensor mechanism of a generic index finger (Fig. 4). While this conjecture has been mentioned in the literature (e.g., [27]–[29]), this is the first study to directly and quantitatively compare alternative 3-D topologies of the extensor mechanism. The specific topology of the Winslow's rhombus tendon network (i.e., the number and connectivity of strings that compose it) we studied is representative of the tendon network of a generic finger dimensioned after our finger models in [29]–[31] (Fig. 3). The input loads to the tendon

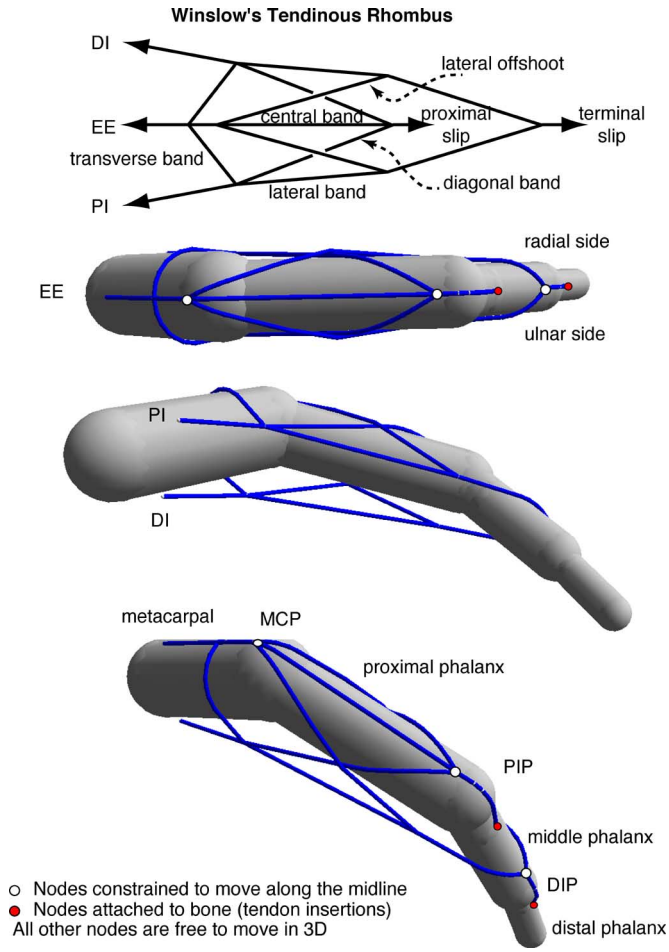


Fig. 3. The 3-D implementation of Winslow's rhombus.

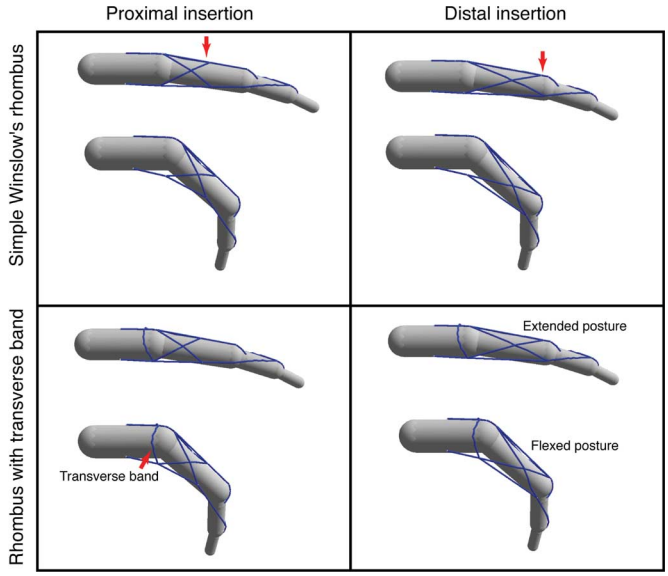


Fig. 4. Two alternative topologies for Winslow's rhombus shown in the "extended" and "flexed" postures simulated. The two topologies differ in the presence or absence of a transverse band (rows in Fig. 3). The more proximal or distal insertion of the diagonal band and lateral offshoot (columns) is a parameter difference.

network are those from an *extrinsic extensor muscle* (EE) such as *extensor digitorum communis* (EC), *dorsal interosseous* (DI), and *palmar interosseous* (PI) muscles. The outputs of the tendon network are the proximal and terminal slips (Fig. 3). Given that the focus of this paper is to investigate the effect of loading on tension propagation through a network of simulated tendons, the following hold. 1) All elastic strings are assigned the same nominal stiffness of 1 GPa, a realistic value from the literature [32], with a radius of 0.5 mm. 2) The nodes defining the finger joints are fixed in space to define the posture studied. The nodes and rods defining the rigid phalanges have a high stiffness of 8 GPa and radii of 10, 8, 6, and 4 mm for the metacarpal, proximal, middle, and distal phalanges, respectively. 3) The bony insertions of DI and EE tendons onto the proximal phalanx are not included because they vary across fingers. 4) The lumbrical muscle is not included because of its small size, its insertion varies across fingers and has its origin in the deep flexor which is not part of the extensor mechanism. For the purposes of this paper, we focus on a longitudinally symmetric network with one input tendon on each side. Passive tissue exists to keep the extensor mechanism centered on the finger. To emulate the passive fascia aligning the tendon network [33], [34], the two nodes defining the central band (shown in white in Fig. 3) are constrained to stay on the midline. All other nodes are free to move in 3-D.

Our chosen topologies either have or are missing the transverse bands connecting the central band to each lateral band (Fig. 3; cf. top and bottom rows in Fig. 4); and have either a relatively proximal or distal insertion for the two cross strings connecting those bands (left and right columns in Fig. 4, respectively). The model without the transverse band is compatible with Winslow's tendinous rhombus (dating from the 17th Century) as described by Zancolli [27], whereas the model with the transverse band was proposed by Garcia-Elias [28] when measuring the tensile properties of the tendinous elements of the extensor mechanism. The more proximal or distal insertions of the diagonal bands and lateral offshoots are varied to find the sensitivity to these yet unknown parameters. In all cases, Winslow's rhombus drape and wrap over the frictionless surface of the finger bones fixed in two functional postures with neutral ad-abduction: the "extended" posture has 10° flexion at all joints and the "flexed" posture has a 45° flexion at the metacarpophalangeal and proximal interphalangeal joints, and a 10° flexion at the distal interphalangeal joint (Figs. 3 and 4).

To study the longitudinally symmetric behavior of the network, we define the following three symmetric loading conditions where there is always at least a 10-N tension at each input tendon simulating muscle tone: i) extensor loading (100 N to EE and 10 N to DI and PI tendons), 2) interosseous loading (10 N to EE and 100 N to DI and PI tendons), and 3) full loading (100 N to each tendon). The maximal simulated applied tension is 100 N, which is compatible with the maximal force generating capacity of the extrinsic extensor and interosseous muscles of the middle finger [34]. The red solid dots on the middle and distal phalanges are the visible portions of the insertion node onto each bone. The simulations compute the resulting tensions in all elements when the network reach equilibrium (within 1 N residual) as per the relaxation solver described previously.

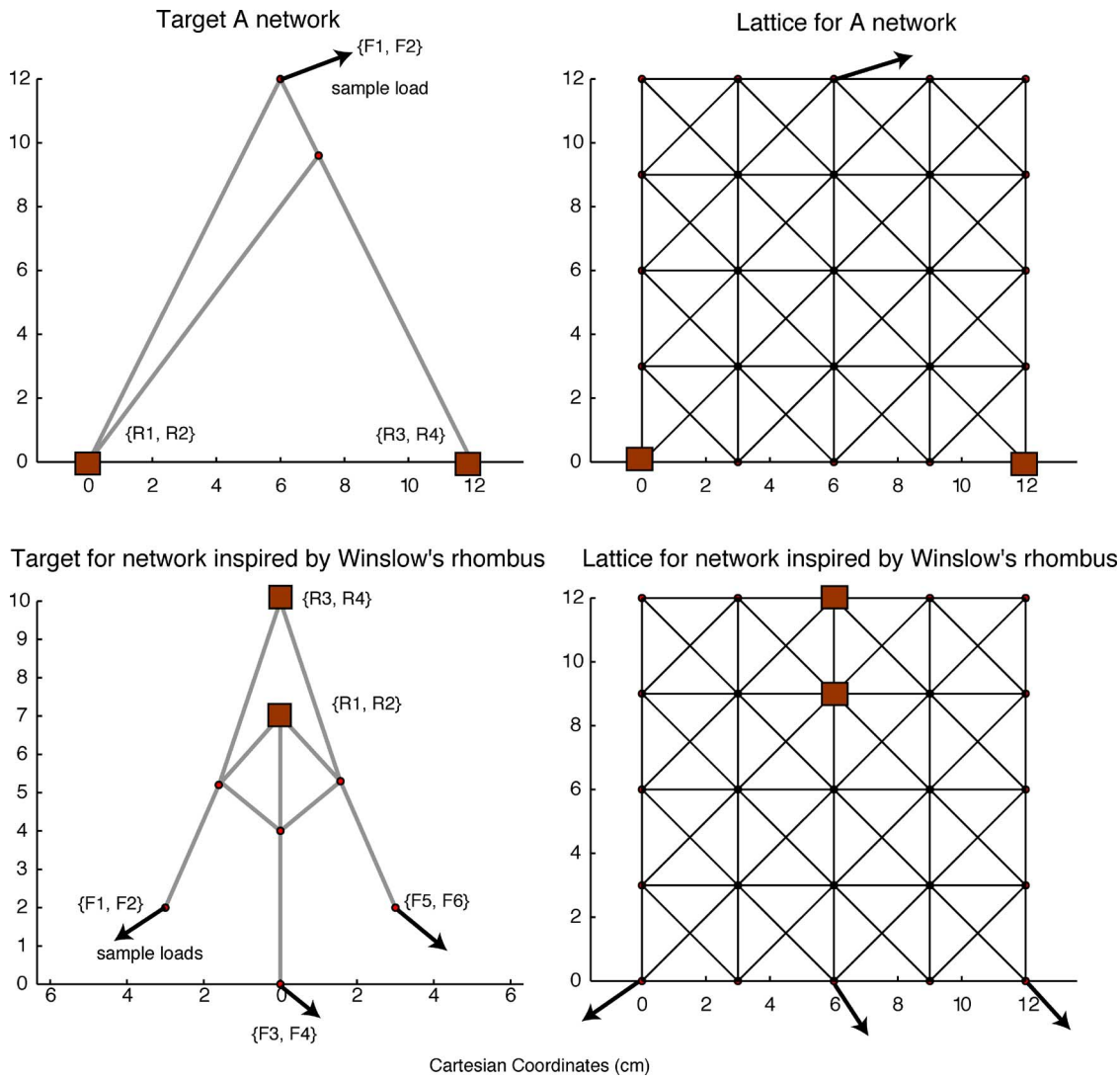


Fig. 5. Evolving two target planar networks. (Top left) A target network of interconnected strings in the shape of the letter "A" and (bottom left) a more complex network inspired by Winslow's rhombus to be evolved from their respective homogenous lattices of strings connected at the nodes (right column). The arrows indicate sample external (input) loads $\{F_x, F_y\}$ at movable nodes, and the square nodes are (output) nodes fixed to ground where reactions forces $\{R_x, R_y\}$ are measured.

D. Inferring a Planar Hidden Network by Searching the Model Space

The goal of this portion of our work is to demonstrate the use of the model inference algorithm to search the model space to infer 2-D models of tendon networks to reproduce input/output data. Inferring the topology and parameters for complex 3-D networks is beyond the scope of this work. Rather, we first tackle the problem of inferring the topology of two planar networks of elastic strings (Fig. 5). The first has an asymmetric shape similar to that of the letter "A" (top of Fig. 5) whose bottom two nodes are grounded and a force is applied to only the topmost node; the applied forces are limited to those with an upward vertical component. The second tendon network is a symmetrical network inspired by Winslow's rhombus [13], [39] where the top two (output) nodes lie along the vertical centerline of the network, correspond to tendon insertions into bone, and are grounded (Fig. 3). External forces are applied to the bottom three (input) nodes; these forces are parallel to the input tendons in their resting configuration and their vertical components are required to be downward. Additionally, the force magnitudes are capped.

For the "A" target, a set of nine systematic tests is run on this network, consisting of all permutations of applied force magnitudes of 0.5, 1.0, and 1.5 with angles of 45°, 90°, and 135° (the angle is measured from the horizontal). After a test, networks are evolved to explain that test and all previous tests. For the network inspired by Winslow rhombus, random tests are chosen. Since the angles of the applied external forces are always chosen to be parallel to the input tendons, a test consists of a set of three force magnitudes. After each randomly designed test, networks are evolved to explain that test and all previous tests.

E. Exploration–Estimation Inference Algorithm: Coevolution of Models and Tests

Last, we present a proof-of-concept initial demonstration of the inference of the hidden topology using sparse, intelligent testing. This approach focuses on using active learning

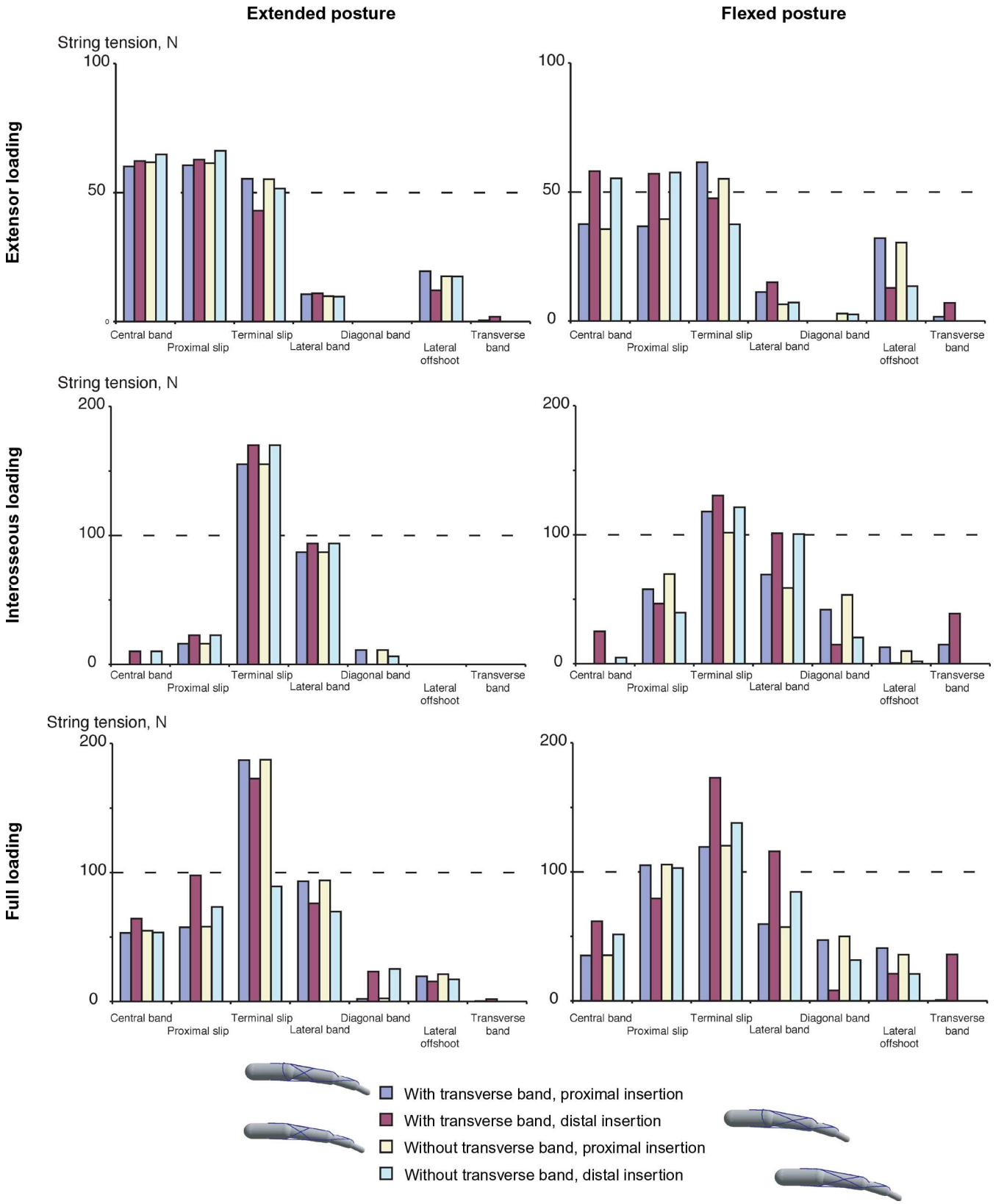


Fig. 6. Effect of topology on the tension distribution through the tendinous network.

methods used successfully in other domains [35], [36], and now used for the inference of biomechanical systems. Briefly, estimation–exploration algorithm [14], [37] we have developed is stochastic, inspired by ideas from evolutionary processes, and in particular, coevolution of two antagonist coexisting populations like predator–prey or host–parasite subecosystems. A schematic of the estimation–exploration algorithm is shown in Fig. 1(c). One population contains 2000 random "candidate

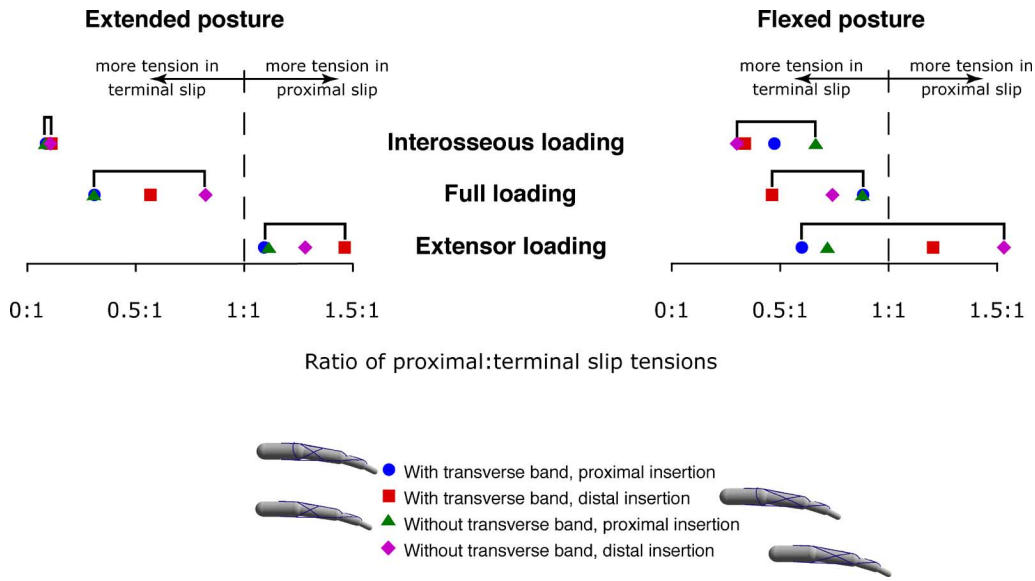


Fig. 7. Effect of topology on the ratio of tensions between the proximal and terminal slips. The relative tensions in the proximal and terminal slips are the defining factor of the possible extension torques that can be produced at the proximal and distal interphalangeal joints, and thus define finger motion and force production capabilities.

tests" (vertical tension at the input nodes, which results in measured reaction forces at the output nodes and locations of the input nodes) to be applied to the target system, while we also have five populations of "candidate models" (networks of elastic strings with the same number of input and output nodes, and location of output nodes; see Sections II-B–II-D). The populations of models are evolutionarily bred by means of variation and selection. The fitness of candidate models is their ability to explain observed data obtained in all experiments so far. The fitness of candidate tests is their ability to create disagreement in the predictions among the fittest models from each of the two populations.

The evolution of candidate models and candidate tests are the estimation and exploration phases, respectively. Each of the two populations of models has 60 candidate models, initially seeded at random. The two populations of models are initially shown the data from a first random test. Thereafter, the populations evolve using Gaussian crossover at 95% and mutation at 5% rates, respectively, until the populations converge (i.e., the fitness of the best model in each population does not change in 150 generations). We take such local convergence as an indication that it is necessary to introduce a new data point (test) to make additional progress. Such new data point will be the product of the next intelligent test, chosen by delivering 2000 random tests to the fittest models from each of the two populations and identifying the test that makes those two models disagree most. Once chosen, the intelligent test is applied to the target system and its resulting data becomes the next data point, in addition to all previous tests, given to the two populations of models to repeat the evolutionary process to reach a new local convergence. Note that after the first iteration the two populations of models are created by combining the best model from the previous iteration with 59 new random models. The progress of the algorithm is quantified by the objective fitness of the models, which is the maximal Euclidean norm of the differences in measured reaction forces plus differences in location of input nodes between the best models and the target network over 100 random tests.

III. Results

In contrast to prior models of the extensor mechanism where tendon tensions are invariant linear functions of input forces, we found—as expected—that tendon tensions are sensitive to network topology, finger posture, and input muscle forces (Fig. 6). For three loading conditions (100 N to EE and 10 N to DI and PI tendons, 10 N to EE and 100 N to DI and PI tendons, or 100 N to each tendon) we found that adding the third tendon changed tendon tensions, on average, $12 \pm 14\%$ (7 ± 11 N) and $31 \pm 44\%$ (8 ± 6 N) for the extended and flexed postures, respectively. Changing the insertion location of the cross strings (a change in a parameter, rather than topology) shows that a more distal insertion changed tendon tensions, on average, $50 \pm 91\%$ (11 ± 14 N) and $52 \pm 43\%$ (19 ± 10 N) for the extended and flexed postures, respectively. Note that Figs. 7 and 8 also show how simultaneous changes in topologies and parameter values lead to substantially different functional predictions.

Of more critical biomechanical relevance, the extension torques the extensor mechanism can produce at the proximal and distal phalangeal joints are also sensitive to topology. Fig. 7 shows how, for each loading condition, the different topologies produce a wide range of relative tension (i.e., extension torques) at the two distal joints of the fingers. The sensitivity is larger for the flexed posture (wider ranges for the interosseous and extensor loading conditions); and in the case of the extensor loading condition, the different topologies lead to reversals in the distribution of tension between the joints (ratios are both $\langle$and$\rangle$ 1).

We evolve a network whose functional behavior and topology resembled the "A" network of Fig. 8 and of a more complex network in Fig. 9. With only one data point, the inference algorithm is, naturally, not able to evolve a network whose topology

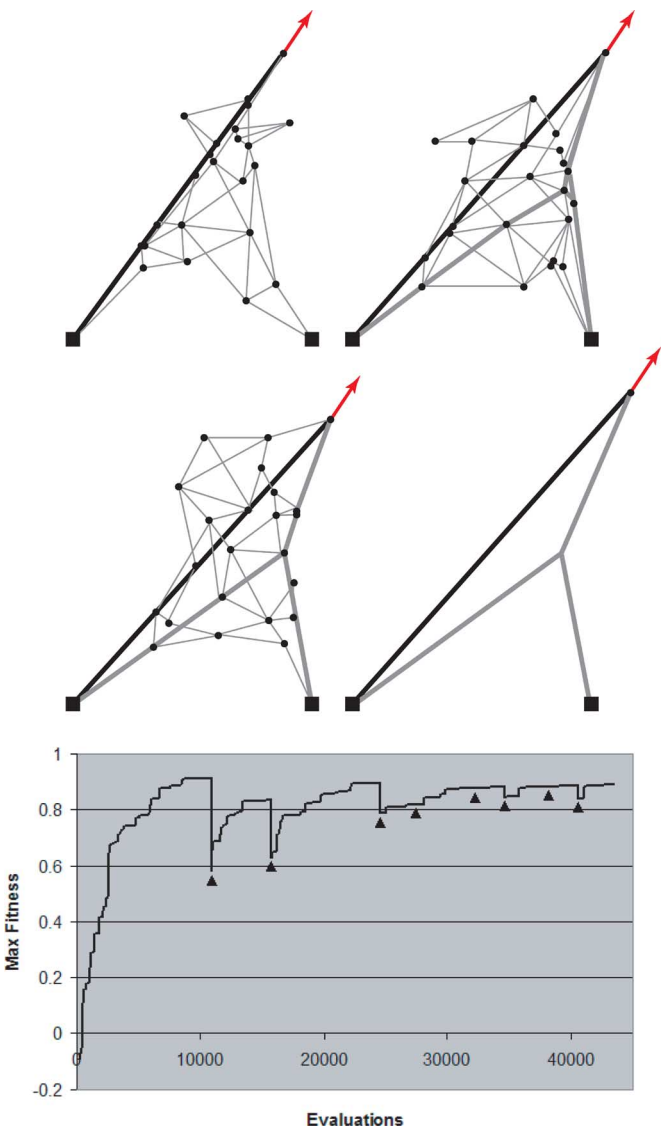


Fig. 8. Top panel: evolution of an "A" network. Top left shows the best network evolved after one test on the target network. Top right shows the best after three tests. Bottom left shows the best after nine tests. Bottom right shows the target network. The intensity of each tendon represents the relative tension carried by it. Bottom Panel: maximal relative fitness of the population versus the number of individuals evaluated for the "A" network. Markers indicate each new test performed on the target system after the relative fitness had reached a plateau for 50 generations (i.e., evaluations).

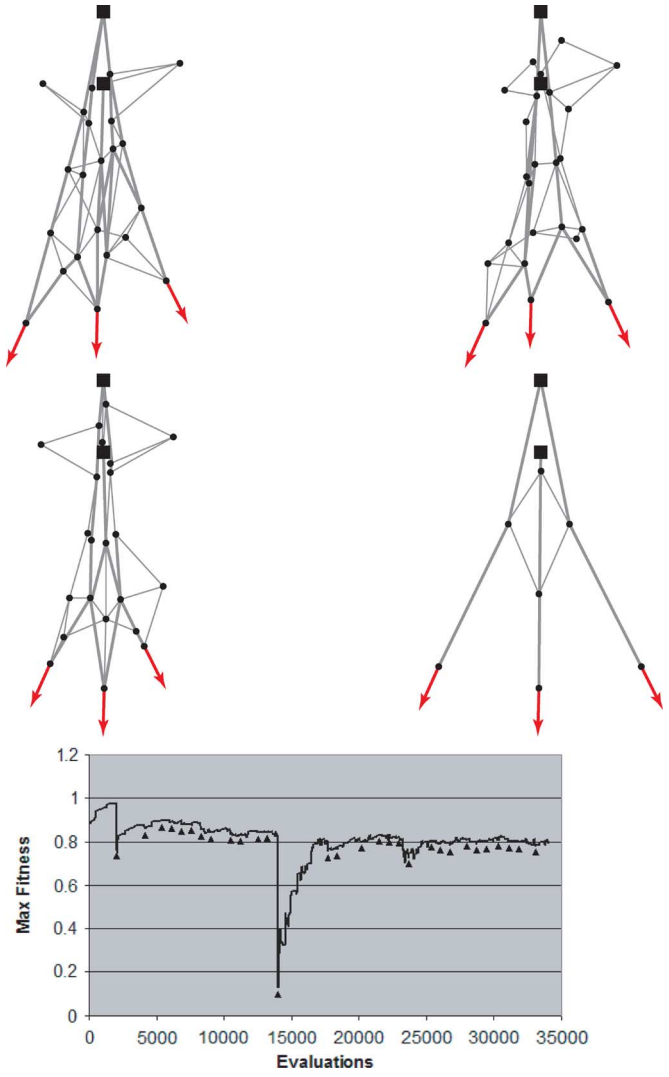


Fig. 9. Top panel: evolution of a complex tendon network inspired by Winslow's rhombus. Top left shows the best network evolved after one test on the target network. Top right shows the best after ten tests. Bottom left shows the best after 30 tests. Bottom right shows the target network. Bottom panel: maximal relative fitness of the population versus the number of individuals evaluated for the complex network. Markers indicate new tests on the target system after the relative fitness had reached a plateau for 50 generations (i.e., evaluations). A large drop in fitness indicates the addition of an informative data point.

resembled that of the target system. However, even after only three (Fig. 8) and ten (Fig. 9) tests on the target system, evolution finds a network whose topology includes key features of the target. Note that the likelihood of a tendon being present is shown by the intensity of its color and the evolved network is similar to the target network. Notice that the top right network in Fig. 8 displays a kink on the right that is characteristic of the target "A" when pulled up and to the right; and that after ten tests on the target system (Fig. 9), the topology of the best network begins to share key topological features with the target network such as the central rhombus and connectivity among nodes. However, the center tendon in the target system that runs from the lower ground to the middle input node is not visible in the fully evolved network, but can be detected using intelligent testing (see Section IV).

Figs. 8 and 9 also show the maximal fitness of the model population versus the number of function evaluations for each network. Markers indicate points where new tests are performed on the target system. Notice that the maximal fitness often drops at these times because new data is made available for fitness calculations. Such tests happen to be the most informative. Performance is measured against the number of network simulations (evaluations) that need to be carried out, as these dominate the *computational cost* of out methods. The number of experimental tests on the target system dominates the *physical cost* of the method.

The estimation–exploration inference algorithm, which focuses on minimizing the physical cost of the method, is able to

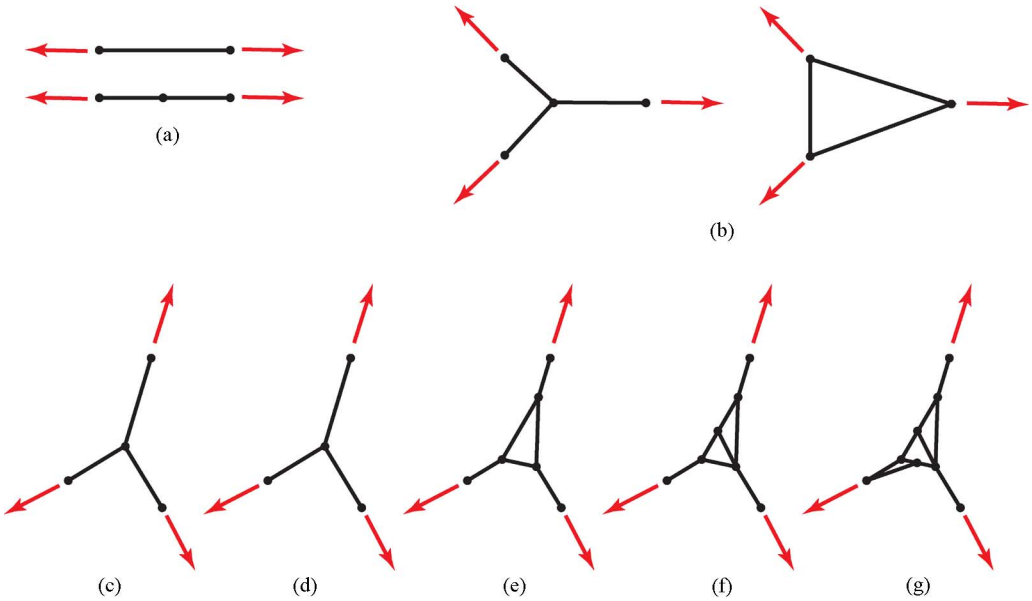


Fig. 10. Separability, observability, and uniqueness of network components and topologies. (a) The 1-D (b) 2-D substructures that can be equivalent under certain parameter settings. These two equivalencies can be used to (c) transform network into (d)–(g) a series of equivalent topologies. Reverse application of these equivalence operators can transform networks (d)–(g) into their canonical form (c).

extract a functionally equivalent and topologically similar network in only 18 tests. Fig. 11 shows the results for these simulations and presents a first demonstration that this method can be statistically better than using random tests.

IV. Discussion

We present critical advances towards the goal of implementing an inference approach to create data-driven biomechanical models by simultaneously inferring both model topology and parameter values. First, we show using a representative 3-D model of a finger that the choice of model topology dramatically affects model predictions. Then, we present the sample test problem of extracting the topology of a hidden planar network of elastic tendons, which is a first step towards solving the notoriously difficult problem of modeling the tendon network of the fingers as a 3-D deformable network of elastic tendons [13], [29]. Specifically, we describe a first-generation computational environment (which we are currently expanding beyond tendon and bone elements) that accounts for a new aspect of biomechanical modeling (explicit exploration of model topology) by using a special static solver (relaxation method) and genetic algorithm (inference algorithm). We show that the estimation algorithm is able to infer functionally equivalent networks that resemble the hidden target network. Last, we introduce an extension that uses the estimation–exploration algorithm to infer the target network with sparse testing. By coevolving populations of candidate model topologies that explain available data and candidate tests to generate data that makes models disagree, the estimation–exploration algorithm shows significantly better convergence than randomly selected tests to recover functionally equivalent representations of a hidden planar tendon network. We conclude by discussing limitations, future directions, as well as model observability and uniqueness.

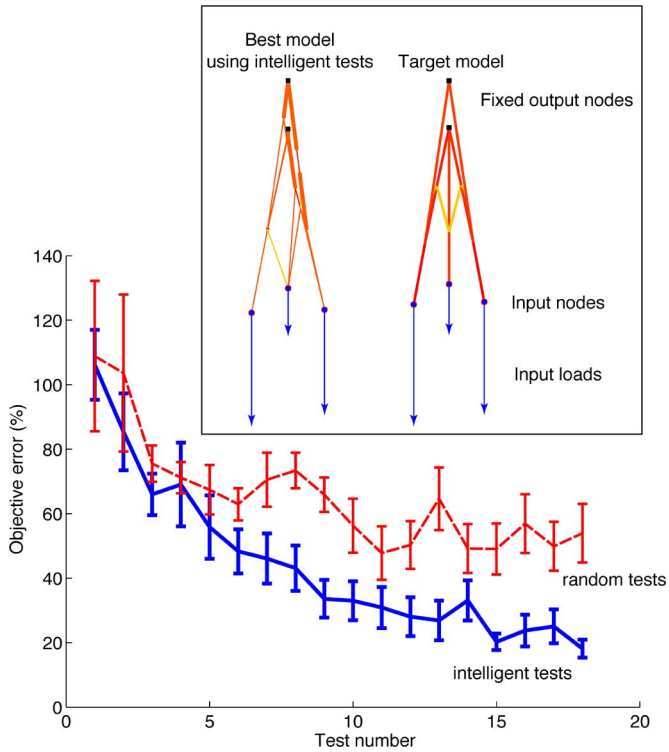


Fig. 11. Statistical trend in objective error for random versus intelligent tests (mean ± SE for ten runs). The estimation–exploration inference algorithm has statistically lower objective error after only six tests ($p < 0.05$ because SE ranges do not overlap) and produces the best model that has a 14% error after 18 tests (see inset). The estimation–exploration inference algorithm was executed ten times (i.e., using intelligent tests) and the mean and standard error for the best model in each run is shown as a solid line. We also executed ten runs using random tests, the results of which (mean and standard error) are shown as a dashed line.

Our simulation environment is particularly well suited to simulate the large deformations in the tendon network of the fingers, as well as everyday manipulation movements that involve low masses and accelerations. To our knowledge, this is the first computational environment that allows automatic descriptions and simulation of anatomical structures that accommodate complex, nonlinear tendinous interconnections wrapped over rigid links, such as those in the extensor mechanism as a function of finger posture and tendon tensions or the tendinous origin of the lumbricals [27], [28], [32], [34], [38]. This quasi-static simulation environment based on a relaxation solver is capable of robustly simulating populations of arbitrary, nonlinear models autonomously generated by our model inference algorithm. More generally, it is a modeling platform that at the moment includes simple building blocks to simulate arbitrary, hinged, or deformable systems consisting of bones, ligaments, tendons, skin, muscles, etc. (a sample is shown in Fig. 2). In this simulator, the physical behavior of the systems emerges from the properties of the building blocks, their topology, and parameter values. To date, we have used this simulator for 2-D (this work) and 3-D tendon networks [29]. Other advantages of this modeling environment are that joints need not be defined by joints, but can be constructed by defining the geometry of the articular surfaces and adding ligaments with the appropriate origin and insertion points. Our future work will continue to extend and validate the building blocks to enable physics-based, causal functional models of arbitrarily complex systems such as the human hand, internal organs, plants, microorganisms, or biological systems living in low-Reynolds numbers regimes.

The relaxation solver itself has several benefits, as follows. 1) It is accurate, as it takes into account large angular changes at joints. This aspect is critical for correct musculoskeletal simulations involving large deformations and angular variations. 2) A relaxation solver accommodates highly nonlinear behaviors, typical of biomechanical tissue (e.g., a tendon is nonlinearly elastic in tension but sustains no load in compression) and can handle multiple entangled chains that are common in many biomechanical systems such as tendon networks, synovial capsules, muscles with multipennate or fanned muscle fibers, etc. 3) It is robust in handling numerical singularities in the biomechanical model (e.g., tendon bifurcations or junctions, sudden tendon loading/unloading) and other biomechanical model instabilities. This is especially important because the biomechanical models that we will be evaluating are iteratively generated by the synthesis algorithm, not by a human, and might occasionally contain local, transient singularities.

While showing that the choice of model topology that affects behavior is not necessarily unexpected, the literature on hand biomechanics to date has not addressed this issue. We have previously shown that the very complexity and deformability of the tendon network of the fingers may be critical to the neural control of manipulation [29] and the present work now enables future detailed exploration of its topology and its functional consequences. As such, these results strongly motivate the systematic search in the model space for topologies for the tendon networks that are compatible with experimental data.

Figs. 8 and 9 demonstrate first examples of the successful inference of the topology of a planar biomechanical model of a tendon network. The computational efficiency and robustness of our simulation environment enable us to explore the model space by coevolving topology and parameter values of candidate models. For computational simplicity, our models in this first example are planar networks of tendons that are first approximations to the functional structure of the tendon networks of the fingers. Future experiments may also evolve the elastic coefficients and cross-sectional areas, as well as other parameters of more sophisticated elements. Our research goals include the further development of our inference algorithm to eventually be able to infer the topology of complex 3-D structures such as those in Figs. 2–4. It is important to make it clear that the applicability of the model inference algorithm is not limited to the use of the quasi-static simulator described here, but rather is amenable for use with any simulation engine such as those for rigid-body dynamics or biochemical models of muscle. The model inference algorithm only needs some simulation engine to predict fitness of a population of models.

Our work naturally has limitations that suggest directions for future work. First, it will be necessary to extend our work to the inference of actual physical systems. This initial validation of a model inference algorithm is based on the target system being a numerical simulation, i.e., a truth-test or hidden-but-known-system approach. This truth-test approach is our necessary first step before we can apply it to inference of the structure of actual cadaver hands by delivering known tensions and excursions to tendons and measuring the forces and motions arising at the finger (for a description of that experimental strategy, see [39]–[41]). By making the topology itself a subject of search, we encounter a number of fundamental questions about the observability, separability, and uniqueness of networks that will shed new light on basic questions about biomechanical modeling. Model inference based on genetic algorithms is computationally costly because increasing the population size of models and tests (Fig. 1) can only be advantageous. In fact, for our future work on inferring models from cadaver tissue, we envision its application as a large-scale parallel computing network that allows the model inference algorithm to propose a next best test every few minutes so that convergence is reached before the unembalmed tissue degrades. Alternatively, when applying similar algorithms to the online inference of networks of neuromuscular control and learning on human subjects, or control strategies for functional electrical stimulation, it will be even more necessary to know the next best test in a matter of seconds. Regarding cross-validation strategies, there are alternative options for using data (e.g., all at once to infer the model topology and then using a second set for cross validation as in surrogate modeling applications). However, here we present the "incremental" approach that corresponds to the real-life case where one wants to perform the fewest tests possible on the (hidden) physical system, and by necessity use data as it becomes available. Future work will need to investigate whether and how the inferred topology depends on the order in which the data points are fed to the algorithm.

Questions concerning "which model is correct" and anatomical variability will be cast more specifically in future work. The inferred models of the two networks we studied are not topologically identical to the target networks, even though they shared key topological features and are functionally equivalent in the sense that the reaction forces for the target and inferred systems are numerically similar. Our model inference algorithm converges to a family of functionally equivalent models that are not identical to each other or to the target network. This means that searching the model space can and does lead to nonunique solutions, likely because having access to only the input/output pairs of data yields an under constrained problem where the observability and separability of the details of the network are limited. This results in the following questions. 1) Can the algorithm be improved to yield unique solutions identical to the target model (e.g., by adding additional reasonable and tenable constraints such as node locations, total area or mass, or cumulative resting length of the topology, etc.)? 2) Can model fitness or convergence be modified to incorporate some aspect of topological uniqueness? 3) Does the inability to infer the exact topology on the basis of input/output data sets is an inherent characteristic of tendon networks or the model space which may have multiple local minima? Thus, our current work will continue along the lines of the detailed exploration of observability, separability, and uniqueness of features of tendon networks. Fig. 10 shows examples of separability, observability, and uniqueness of network components. The issue of functional equivalence and observability is critical to the development of this kind of physics-based, causal models because they will be most useful clinically when they can infer specific anatomical structures associated with observed function (e.g., whether lengthening, shortening, or replacing some specific tendon, muscle, ligament, skin patch, tendon pulley, etc., will lead to a desirable functional outcome). In contrast to modeling approaches such as, say, neural networks that provide a mathematical mapping of inputs to outputs, we prefer to propose to develop modeling approaches capable of providing biomechanical insight. Thus, we will continue to work on an approach based on building blocks and topological rules that are physics-based and very much emulating functional anatomy.

Specifically, with respect to modeling the hand, the tools and approaches have not changed much since the 1960s and 1970s when An, Chao, Brand, Tubiana, and others first proposed a biomechanical approach to this complex system. In [29], we describe how the function of tendon networks has been debated since the time of Vesalii and DaVinci [27], [42], [43], and how the very "complexity" of the system may be an important example of brain-body coevolution that enhances the biomechanical function of the fingers in ways not possible with "simple" tendon paths from muscle to bone. That prior work and the present results showing sensitivity to assumed topology of the tendon network suggest that detailed modeling of the anatomy of the hand and our understanding of its neuromuscular control are still in their infancy. For example, our results inferring functionally equivalent networks to Winslow's rhombus suggests we may need to rethink whether the tendon network of the fingers has "crossover" tendons (i.e., with the diagonal band and lateral offshoot sliding past each other; Fig. 3). Winslow's anatomy book published in 1732 has no illustrations [43] (a copy exists at Cornell University's Koch Library Division of Rare and Manuscript Collections). The first graphical descriptions of Winslow's rhombus were by Zancolli in 1979 [27] and Chao and An who draw it with crossover tendons as in Fig. 3 [1]. By showing functionally equivalent networks that do not include such crossover tendons, our results suggest future work to establish whether tendon networks with crossover tendons are observable, separable, or unique. Representations without crossover tendons may be more anatomically tenable because they prevent sliding and rubbing that may induce damage to the tendon sheaths and lead to adhesions. In fact, a detailed dissections of the extensor mechanism shows how the graphical description in Fig. 3 is more of a functional diagram than a model (see anatomical drawings in, for example, [27], [28], [44], and [45]) because clear and independent crossover tendons are not easily seen.

We conclude by showing a simple example of the estimation–exploration inference algorithm to begin to address the questions of whether it is possible to use fewer, more informative, tests to avoid unnecessary interrogations of the target system. While many machine learning and bioinformatics methods are data intensive, biological systems can often provide only a limited amount of data because of cost, difficulty, time, risk, availability of samples, fragility or because the properties of the system may change over time. Thus, methods that can perform system identification on biological systems with sparse interrogation are necessary for certain classes of problems. This algorithm offers an online, data-sparse approach, as an alternative to traditional batch (offline) data-intensive bioinformatics approaches, and is thus much more suitable for the inference of *in vitro* and *in vivo* biomechanical systems. This concept significantly reduces the number of tests in a number of other problem domains including inference of robot kinematic structures, inference of gene-regulation networks, and inference finite-state machines [14], [37]. Fig. 11 shows that implementing the estimation–exploration algorithm is feasible and better than using an equivalent number of random tests. Based on these encouraging first results, we will continue to compare this novel algorithm to other active model extraction methods.

REFERENCES

[1] K. N. An, E. Y. Chao, W. P. Cooney, and R. L. Linscheid, "Normative model of human hand for biomechanical analysis.," *J. Biomech.*, vol. 12, pp. 775–788, 1979.

[2] H. J. Sommer and N. R. Miller, "A technique for kinematic modeling of anatomical joints," *J. Biomech. Eng.*, vol. 102, pp. 311–317, 1980.

[3] F. E. Zajac, "Muscle and tendon: Properties, models, scaling, and application to biomechanics and motor control," *Crit. Rev. Biomed. Eng.*, vol. 17, pp. 359–411, 1989.

[4] S. L. Delp, J. P. Loan, M. G. Hoy, F. E. Zajac, E. L. Topp, and J. M. Rosen, "An interactive graphics-based model of the lower extremity to study orthopaedic surgical procedures," *IEEE Trans. Biomed. Eng.*, vol. 37, no. 8, pp. 757–767, Aug. 1990.

[5] V. J. Santos and F. J. Valero-Cuevas, "Reported anatomical variability naturally leads to multimodal distributions of Denavit-Hartenberg parameters for the human thumb," *IEEE Trans. Biomed. Eng.*, vol. 53, no. 2, pp. 155–163, Feb. 2006.
[6] F. J. Valero-Cuevas, M. E. Johanson, and J. D. Towles, "Towards a realistic biomechanical model of the thumb: The choice of kinematic description may be more critical than the solution method or the variability/uncertainty of musculoskeletal parameters," *J. Biomech.*, vol. 36, pp. 1019–1030, 2003.
[7] A. van den Bogert, K. Gerritsena, and G. Cole, "Human muscle modelling from a user's perspective," *J. Electromyogr. Kinesiol.*, vol. 8, pp. 119–124, 1998.
[8] A. J. van den Bogert, G. D. Smith, and B. M. Nigg, "In vivo determination of the anatomical axes of the ankle joint complex: An optimization approach," *J. Biomech.*, vol. 27, pp. 1477–1488, 1994.
[9] E. Alpaydin, *Introduction to Machine Learning*. Cambridge, MA: MIT Press, 2004.
[10] K. Kozlowski, *Modelling and Identification in Robotics*. New York: Springer-Verlag, 1998.
[11] L. Ljung, *System Identification: Theory for the User*, 2nd ed. Upper Saddle River, NJ: Prentice-Hall, 1999.
[12] F. J. Valero-Cuevas and H. Lipson, "A computational environment to simulate complex tendinous topologies," presented at the 26th Annu. Int. Conf. IEEE Eng. Med. Biol. Soc., San Francisco, CA, 2004, unpublished.
[13] F. J. Valero-Cuevas, "An integrative approach to the biomechanical function and neuromuscular control of the fingers," *J. Biomech.*, vol. 38, pp. 673–684, 2005.
[14] J. C. Bongard and H. Lipson, "Topological system identification using coevolution of models and tests," *IEEE Trans. Evol. Comput.*, vol. 9, no. 4, pp. 361–384, Aug. 2005.
[15] H. Lipson, E. K. Antonsson, and J. R. Koza, "Computational synthesis: From basic building blocks to high level functionality," in *Proc. Assoc. Adv. Artif. Intell. Symp.*, Menlo Park, CA, 2003, pp. 24–31, ISBN: 1-57735-179-7.
[16] V. Anand, H. Lipson, and F. Valero-Cuevas, "Blind inference of nonlinear cable network topology from sparse data," presented at the GECCO: Genetic Evolut. Comput. Conf., Washington, DC, 2005, unpublished.
[17] W. G. Darling and K. J. Cole, "Muscle activation patterns and kinetics of human index finger movements," *J. Neurophysiol.*, vol. 63, pp. 1098–1108, 1990.
[18] D. G. Kamper, T. G. Hornby, and W. Z. Rymer, "Extrinsic flexor muscles generate concurrent flexion of all three finger joints," *J. Biomech.*, vol. 35, pp. 1581–1589, 2002.
[19] D. C. Harding, K. D. Brandt, and B. M. Hillberry, "Finger joint force minimization in pianists using optimization techniques," *J. Biomech.*, vol. 26, pp. 1403–1412, 1993.
[20] K. J. Cole and J. H. Abbs, "Coordination of three-joint digit movements for rapid finger-thumb grasp.," *J. Neurophysiol.*, vol. 55, pp. 1407–1423, 1986.
[21] H. J. Buchner, M. J. Hines, and H. Hemami, "A dynamic model of finger interphalangeal coordination," *J. Biomech.*, vol. 21, pp. 459–468, 1988.
[22] A. Esteki and J. M. Mansour, "An experimentally based nonlinear viscoelastic model of joint passive moment," *J. Biomech.*, vol. 29, pp. 443–450, 1996.
[23] H. Lipson and J. B. Pollack, "Automatic design and manufacture of robotic lifeforms," *Nature*, vol. 406, pp. 974–978, 2000.
[24] H. Lipson, "A relaxation method for simulating the kinematics of compound nonlinear mechanisms," *ASME J. Mech. Design*, vol. 128, pp. 719–728, 2006.
[25] H. Lipson and J. C. Bongard, "An exploration-estimation algorithm for synthesis and analysis of engineering systems using minimal physical testing," presented at the ASME Design Autom. Conf., Salt Lake City, UT, 2004, unpublished.
[26] S. W. Mahfoud, *Niching Methods for Genetic Algorithms*. Urbana-Champaign, IL: Univ. Illinois Urbana-Champaign, 1995.
[27] E. Zancolli, *Structural and Dynamic Bases of Hand Surgery*, 2nd ed. Philadelphia, PA: Lippincott, 1979.
[28] M. Garcia-Elias, K. N. An, L. Berglund, R. L. Linscheid, W. P. Cooney, and E. Y. Chao, "Extensor mechanism of the fingers: I. A quantitative geometric study," *J. Hand Surgery (American)*, vol. 16, pp. 1130–1140, 1991.
[29] F. J. Valero-Cuevas, J. W. Yi, D. Brown, R. V. McNamara, III, C. Paul, and H. Lipson, "The tendon network of the fingers performs anatomical computation at a macroscopic scale," *IEEE Trans. Biomed. Eng.*, vol. 54, no. 6, pt. 2, pp. 1161–1166, Jun. 2007.
[30] F. J. Valero-Cuevas, F. E. Zajac, and C. G. Burgar, "Large index-fingertip forces are produced by subject-independent patterns of muscle excitation," *J. Biomech.*, vol. 31, pp. 693–703, 1998.
[31] F. J. Valero-Cuevas, "Predictive modulation of muscle coordination pattern magnitude scales fingertip force magnitude over the voluntary range," *J. Neurophysiol.*, vol. 83, pp. 1469–1479, 2000.
[32] M. Garcia-Elias, K. N. An, L. J. Berglund, R. L. Linscheid, W. P. Cooney, and E. Y. Chao, "Extensor mechanism of the fingers: II. Tensile properties of components," *J. Hand Surgery (American)*, vol. 16, pp. 1130–1140, 1991.
[33] R. Tubiana, *The Hand*. Philadelphia, PA: Saunders, 1981, vol. 1, p. 753.
[34] P. Brand and A. Hollister, *Clinical Mechanics of the Hand*, 3rd ed. St. Louis, MO: Mosby-Year Book, 1999.
[35] B. Kouchmeshky, W. Aquino, J. C. Bongard, and H. Lipson, "Co-evolutionary algorithm for structural damage identification using minimal physical testing," *Int. J. Numer. Methods Eng.*, vol. 69, no. 5, pp. 1085–1107, Jan. 2007.
[36] V. Zykov, E. Mytilinaios, B. Adams, and H. Lipson, "Robotics: Self-reproducing machines," *Nature*, vol. 435, pp. 163–164, 2005.
[37] J. Bongard, V. Zykov, and H. Lipson, "Resilient machines through continuous self-modeling," *Science*, vol. 314, pp. 1118–1121, 2006.
[38] S. Bunnell, *Surgery of the Hand*. Philadelphia, PA: Lippincott, 1944.
[39] F. J. Valero-Cuevas, J. D. Towles, and V. R. Hentz, "Quantification of fingertip force reduction in the forefinger following simulated paralysis of extensor and intrinsic muscles," *J. Biomech.*, vol. 33, pp. 1601–1609, 2000.
[40] F. J. Valero-Cuevas and V. R. Hentz, "Releasing the A3 pulley and leaving flexor superficialis intact increase palmar force following the Zancolli lasso procedures to prevent claw deformity in the intrinsic minus hand," *J. Orthopaedic Res.*, vol. 20, pp. 902–909, 2002.
[41] J. L. Pearlman, S. S. Roach, and F. J. Valero-Cuevas, "The fundamental thumb-tip force vectors produced by the muscles of the thumb," *J. Orthopaedic Res.*, vol. 22, pp. 306–312, 2004.
[42] A. Vesalii, *De humani corporis fabrica libri septem*. Brussels: Belgium, 1543.
[43] J. B. Winslow, *Exposition anatomique de la structure du corps humain*. Paris, France: Guillaume Desprez et Jean Desessarte, 1732.
[44] Y. Ikebuchi, T. Murakami, and A. Ohtsuka, "The interosseous and lumbrical muscles in the human hand, with special reference to the insertions of the interosseous muscles," *Acta Med. Okayama*, vol. 42, pp. 327–334, 1988.
[45] F. H. Netter, *Atlas of Human Anatomy*, 2nd ed. Yardley, PA: Icon Learning Systems, 1997.



Francisco J. Valero-Cuevas (M'99) received the B.S. degree in engineering from Swarthmore College, Swarthmore, PA, in 1988, the M.S. degree from Queen's University, Kingston, ON, Canada in 1991, and the Ph.D. degree from Stanford University, Stanford, CA, in 1997, both in mechanical engineering.

He was an Assistant and Associate Professor at the Sibley School of Mechanical and Aerospace Engineering, Cornell University, Ithaca, NY, and an Associate Professor of Applied Biomechanics at Cornell's Weill Medical College. Currently, he is an Associate Professor at the Department of Biomedical Engineering and the Division of Biokinesiology and Physical Therapy, University of Southern California, Los Angeles. His research interests focus on combining engineering, robotics, mathematics and neuroscience to understand organismal and robotic systems for basic science, engineering and clinical applications.

Prof. Valero-Cuevas is member of the IEEE Engineering in Medicine and Biology Society, the American and International Societies of Biomechanics, the American Society of Mechanical Engineers, the Society for Neuroscience, and the Society for the Neural Control of Movement. He has received a Research Fellowships from the Alexander von Humboldt Foundation in 2005, the Postdoctoral Young Scientist Award from the American Society of Biomechanics in 2003, the Faculty Early Career Development Program CAREER Award from the National Science Foundation in 2003, the Innovation Prize from the State of Tyrol in Austria in 1999, a Fellowship from the Thomas J. Watson Foundation in 1988, and was elected Associate Member of the Scientific Research Society Sigma-Xi in 1988. He serves as an Associate Editor for the IEEE TRANSACTIONS ON BIOMEDICAL ENGINEERING.



Vikrant V. Anand received the S.B. degree in mechanical engineering from the Massachusetts Institute of Technology, Cambridge, in 1995 and the MBA degree in finance from Carnegie Mellon University, Pittsburgh, PA, in 2000. Currently, he is working towards the Ph.D. degree in accounting and economics at the Johnson Graduate School of Management, Cornell University, Ithaca, NY.

He was a Graduate Research Assistant at the Department of Mechanical and Aerospace Engineering, Cornell University. He was also a Management Consultant for Deloitte Consulting and for Science Applications International Corporation and an Engineer for the Ford Motor Company.



Anupam Saxena received the B.S. degree in mechanical engineering from the Indian Institute of Technology, Bombay, India, in 1995, the M.S. degree in mechanical engineering from the University of Toledo, Toledo, OH, in 1997, and the Ph.D. degree in mechanical engineering and applied mechanics from University of Pennsylvania, Philadelphia, in 2000.

He is a member of the Mechanical Engineering Faculty at the Indian Institute of Technology, Kanpur, India, and is currently a Visiting Assistant Professor at the Sibley School of Mechanical and Aerospace Engineering Department, Cornell University, Ithaca, NY. He has 12 archival and accepted publications, numerous proceedings, and has coauthored a book "Computer Aided Engineering Design" (Springer-Verlag: Dordrecht, The Netherlands, 2005). His research interests focus on the nature and design of compliant and robotic systems (CARS). He has worked on topological synthesis of compliant mechanisms with applications in microelectromechanical systems (MEMS). This includes synthesis of optimal fully compliant continua for variety of applications involving nonlinear output paths, energy efficient displacement transduction (amplification or inversion), and failure criteria (safety factor based and stress constraints based). He has implemented topology, shape, and size synthesis with both discrete (cells with frame elements) and continuum (honeycomb arrangement) representations employing mathematical programming and evolutionary computation techniques. In robotics, he has worked on optimal trajectory planning of bipeds with soft sole, and optimal arrest of gradually moving objects through projective path planning with multiagents.



Hod Lipson (M'98) received the B.Sc. degree in mechanical engineering and the Ph.D. degree in mechanical engineering in computer-aided design and artificial intelligence in design from The Technion—Israel Institute of Technology, Haifa, Israel, in 1989 and 1998, respectively.

Since 2001, he has been an Assistant Professor at the Mechanical and Aerospace Engineering and Computing and Information Science Schools, Cornell University, Ithaca, NY. Prior to this appointment, he was a Postdoctoral Researcher at the Brandeis University's Computer Science Department and a Lecturer at the Mechanical Engineering Department, Massachusetts Institute of Technology, Cambridge, where he conducted research in design automation. His research interests focus on computational methods for synthesizing complex systems out of elementary building blocks and the application of such methods to design automation and their implication to understanding the evolution of complexity in nature and in engineering.